The shape of spiral galaxies

Author: Esperanza Mur Arellano
Facultat de Física, Universitat de Barcelona, Diagonal 645, 08028 Barcelona, Spain.

Advisor: Maria Teresa Antoja Castelltort

Abstract: In this work we analyze the stellar surface density distribution in the equatorial plane of the disk of a spiral galaxy from a cosmological simulation and its evolution. We apply a Fourier series adjustment that allows us to detect the different internal structures of the galaxy and intuitively interpret them as central bars, spiral arms or lopsidedness. We see that the galaxy has a complex structure, but it is dominated by the first two Fourier modes, giving rise to a central bar and a spiral arm that winds around the galaxy from the middle radii to outwards. These present different rotation frequencies and, in general, their relative amplitudes increase with the passage of time. The cause of this could be the influence of the satellites, the consequence of the deformation of the halo or the result of the gas accretion, but this should be studied more carefully in the future.

I. INTRODUCTION

Galaxies have historically been classified according to their shape into three large groups: disk galaxies (widely known as spiral galaxies, and which represent approximately 70% of the total number of galaxies known today), elliptical galaxies, and irregular galaxies. Focusing on the first category, these usually present a circular distribution with internal structures such as central bars and spiral arms that make the surface stellar density of the galaxy disk not uniform. Another type of non-isotropic density distribution is the lopsidedness (i.e. the surface density of the galaxy is higher on one side than the other). This phenomenon is not at all isolated and, in fact, it has been seen that, studying a sample of spiral galaxies, about 30% of them present considerable lopsidedness [1].

There are various causes for the appearance of lopsidedness in a galaxy and they are still being studied (for a detailed description, see the review of Jog & Combes [5]). One of them is the gravitational force exerted by satellite galaxies when approaching the main galaxy [2]. This would lead to an off-centering of the stellar distribution that would readjust over time. Another important cause is the influence of the shape of the heavy dark halo [11], since its supposed triaxiality would produce a deformation on the galaxy. There are also other possible causes to consider such as gas accretion [4].

To this day, different studies of galactic structures and their imbalances have been carried out. Most of them are based on N-body simulations, although there are also some cases from cosmological simulations (for example, a study made from a simulation that only includes dark matter and uses recipes to create the stars [3], or another made with a more complex simulation but only focused on the interstellar gas [9]). As far as we know, lopsidedness has not yet been studied with complex simulations that include DM, stars and gas, as we do here.

There is still a long way to go as the exact causes of the imbalance are not yet clear since we have a wide range of possibilities. Thus, our objective is to analyze the evolution of the lopsidedness and the dominant structures of a galaxy from a complex cosmological simulation that allows us to obtain more realistic results. To quantify the phenomena we use the Fourier series adjustment method.

In Sect. 2 we talk about the methodology used to carry out the analysis, in Sect. 3 we show the obtained results and in Sect. 4 we give the conclusions of the work.

II. METHODOLOGY

A. Simulation

To carry out our study of the lopsidedness in galactic disks and its evolution over time, we perform an analysis of the stellar density distribution in the equatorial plane of the disk in a simulation. In particular, we use the GARROTXA set of cosmological simulations [8]. This reproduces the evolution of Milky Way-mass galaxies taking into account stars, dark matter, and interstellar gas. We focus on the study of a MW-type system that has a mass assembling history similar to that of the real MW and, specifically, we analyze the behavior at low-z. It should be noted that the simulated galaxies are in a complex environment with multiple satellites, tidal streams, etc. Furthermore, the simulation has sufficient temporal and spatial resolution so that we can study the dynamics of the disk and its temporal evolution in detail.

We start from a set of quantities for each simulated particle (position, velocity, age, etc) that characterize the state and distribution of the “stars” that we study at a certain moment in the Universe, which we call snapshots. Each snapshot is centered on the center of mass of the galaxy and aligned so the vertical axis is directed along the disk vertical dimension. We use cylindrical coordinates, r, ϕ, z, since the distribution has a naturally flattened cylinder shape. We work on two frames of reference: the first is fixed on the central bar of the galaxy (which we refer to as the fixed bar frame and which allows us to see how the structures behave with respect to the central bar) and the second is the inertial frame, IRF.

Each of these snapshot is characterized by a scale factor, a, which allows us to easily identify them and which we can translate to lookback time. It should be said that we speak of "stars" instead of literally stars because, due to the limitations of computational calculation, each particle in the simulation (for which the quantities are obtained) is not exactly a star, but represents a group of stars born out of a single localized star formation event.

B. Lopsidedness quantification

To understand the behavior and causes of disk imbalance, we must find some way to quantify it. Since there is no single way to do this, we tested different approaches during this study. We first thought of studying the deviation of the geometric center of the galaxy from the center of mass by delimiting a boundary for the galaxy and fitting the stellar surface density to a cylindrical radius exponential decay function. We also thought about analyzing the means of the coordinates r and ϕ for each of the concentric circular rings into which we would have previously divided the galaxy. As we move forward with these ideas, we began to observe interesting behaviors but we ruled out continuing with these methods because they were yielding slightly noisy results and we needed a concise method that allow us to do a deeper analysis.

Finally, we decided to perform a Fourier series decomposition for the distribution of stars as a function of the azimuth angle of their position in the galaxy. To do this, we divide the galaxy into concentric circular rings (the center of these being the center of mass of the galaxy) and we apply the decomposition to each of them. We opted for this option since we achieve a clear and intuitive quantification of the different modes that can characterize a galaxy density distribution.

C. Fourier series fit method

To approximate a certain distribution with a Fourier series fit (in this case the azimuth angle profile), we model it according to:

$$I_0(r,\phi) = I_0 + \sum I_{mc}(r)cos(m\phi) + \sum I_{ms}(r)sin(m\phi). \quad (1)$$

The Fourier terms presented in this expression are calculated as in [6]:

$$I_0(r) = < I(r,\phi) > \quad (2)$$

$$I_{mc}(r) = 2 < I(r,\phi)cos(m\phi) > \quad (3)$$

$$I_{ms}(r) = 2 < I(r,\phi)sin(m\phi) > \quad (4)$$

where m is an integer denoting the Fourier mode. With all this, we can interpret the modes in a very graphic and intuitive way:

- Mode 1 corresponds to finding a single maximum and a single minimum per 2π period in the distribution. This can be the case of the galaxy having a certain lopsidedness or one single spiral arm (lopsidedness with azimuthal dependence).
- Mode 2 corresponds to finding two maximums and two minimums in a period. This may correspond to the fact that the galaxy has a structure formed by 2 spiral arms or that the distribution of the stars in the equatorial plane has an elliptical shape due a central bar or to an elliptical disk.
- Following the same logic for the higher modes, a mode m would describe a distribution formed by an m symmetry.

We can calculate the amplitudes and phases (azimuth angles for which the Fourier decomposition density is maximum) of each mode for each ring according to:

$$A_m(r) = \sqrt{I_{mc}(r)^2 + I_{ms}(r)^2}/I_0(r) \quad (5)$$

$$\phi_m = (1/m)\tan^{-1}(I_{ms}/I_{mc}). \quad (6)$$

Notice that, since the definition of the amplitudes corresponding to modes other than 0 includes a factor 2, the relative amplitude can be up to 2. This would be an exceptional case and, hereinafter, we work with amplitudes whose magnitude rarely exceed 1.

III. RESULTS

In this section we present our results. In Sect. A we analyse a single time in the evolution of the simulated galaxy that also serves us as a good illustration of our methodology and in Sect. B we analyze the Fourier decomposition for the full temporal evolution of the model.

A. Analysis of a single snapshot

To illustrate the method, we show its application for the snapshot corresponding to $a = 0.950$ (lookback time of 0.73 Gy). In order to appreciate the modes as clearly as possible, we choose a subset of star particles to enhance them. We select a population with ages between 0 and 5 Gy (since older populations are usually less affected by disturbances) and we divide it into rings with a radius of 1 kpc. Furthermore, we limit ourselves to the equatorial plane of the galactic disk, such that $|z| < 6$ kpc. We carry out the Fourier development up to order 4, since we have seen that the contribution of higher orders is notably less relevant. Now, let's see how the Fourier fit adjusts with respect to the real distribution of the azimuth angle. Although we calculated the fit for the entire galaxy, we only show the plots of a pair of rings in which a particular mode can be seen clearly (Fig. 1).

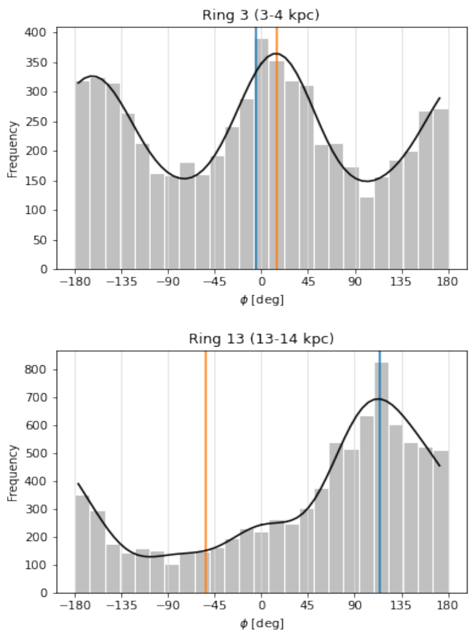

FIG. 1: Azimuth angle distribution (histogram) and its adjustment by Fourier series to order 4 (black line). The blue vertical line represents the mode 1 phase and the orange one shows the mode 2 phase. Each panel corresponds to a ring on the disk: ring 3 in the upper panel and ring 13 in the lower one (lookback time: 0.73 Gy).

The general observation about Fig. 1 is that the Fourier fit up to order 4 (black line) adjusts the behavior of our azimuthal distribution (grey histogram) quite precisely. Now, speaking of the rings shown, in ring 3 the mode 2 dominates and the distribution, to which the Fourier fit adjusts very sinusoidally, has two maximums and two minimums (one of which coincides with the Fourier phase angle of mode 2 obtained by the method and shown in orange). In the case of ring 13 the mode 1 is dominating and the well-defined distribution has one maximum and one minimum (again agreeing the position of the maximum amplitude with that of the Fourier phase angle of mode 1 in blue) and a very satisfactory Fourier fit.

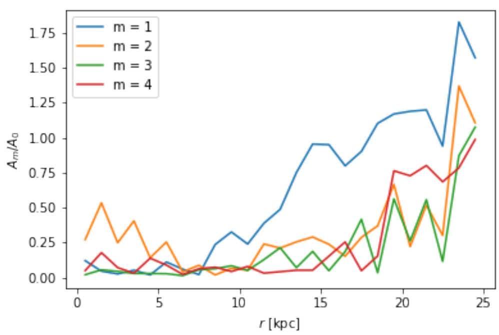

FIG. 2: Fourier relative amplitudes for the 4 first and more relevant modes as a function of the galaxy radius (lookback time: 0.73 Gy).

In Fig. 2 we present the Fourier relative amplitudes for the first modes as a function of the galaxy radius. Mode 2 dominates in the innermost radii while, as we move away from the center, this contribution loses strength and that of mode 1 gains it. Since these are the dominant modes, from this point on, we focus on them and leave higher orders aside. From about $r = 20$ kpc, there are so few stars per ring that the results are significantly noisy.

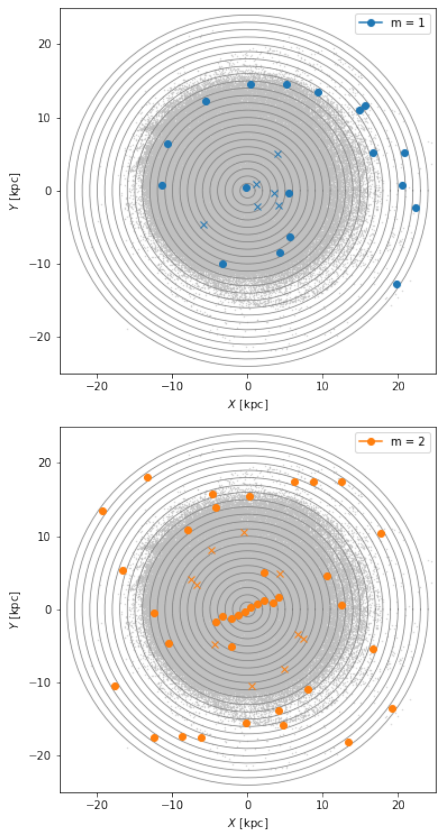

FIG. 3: Fourier phase angle represented for each ring on the equatorial plane of the galaxy. The mode 1 is shown in the upper panel (blue) and the mode 2 is shown in the lower one (orange). Crosses are rings where the relative amplitude is smaller than 10%, while filled circles are for larger amplitudes (lookback time: 0.73 Gy).

The Fourier representation can be observed in a more intuitive way by plotting the Fourier phase angle for each ring on the equatorial plane of the galaxy (Fig. 3). Remembering that the position of the phase angle gives us, by definition, the point of maximum amplitude of the decomposition of a certain mode, we can roughly deduce what type of structures make up the galaxy at each radius. On the one hand, we find a spiral arm associated with mode 1 towards the outskirts (upper panel) and, on the other, a central bar associated with the mode 2 and some hints of a 2-armed structures (lower panel).

After exploring the results for a single snapshot, now we proceed to analyze the evolution of the lopsidedness with time by applying the method to all snapshots.

B. Fourier decomposition for all the galaxy evolution

In order to analyze the behavior of the two main modes, we elaborated a set of plots that allow us to see the evolution in time of the relative amplitudes and the phases for different radii (Fig. 4 and Fig. 5), whose values are indicated by the color of their representation on the plot. We do this automatically for all snapshots and for the same subset of stars as in the case of a single snapshot (ages between 0 to 5 Gy and $|z| < 6$ kpc). Now, let's describe the observed results for each mode, from the center of the galaxy outwards (since we found a very complex disk, we focus on the most obvious structures).

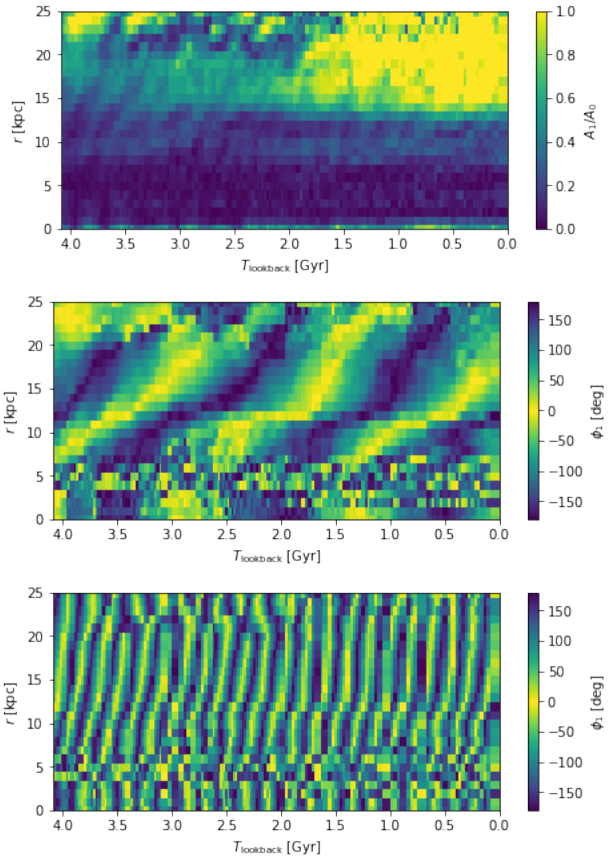

FIG. 4: Fourier relative amplitudes (upper panel) and the Fourier phase angles (middle and lower panels), as a function of lookback time, for each radius and for mode 1. For the phase representation, we distinguish one panel for the point of view of the fixed bar frame (middle panel) and another for the IRF one (lower panel). Also for the phase representation, we have defined the color bar in such a way that the color pattern is cyclical for a more intuitive interpretation of the phases behaviour.

- Mode 1 (Fig. 4): in the innermost radii of the galaxy ($r < 1$ kpc) we see a mode 1 structure that could be a nuclear disk whose phase angle evolves with time, thus, it is rotating with respect to the central bar (middle panel). Between $r = 2$ kpc and $r = 7$ kpc, we find a zone of very low amplitudes and, around $r = 5$ kpc, there is a significant amount of noise in the phases. Beyond 7 kpc, we observe a non-negligible amplitude and a coherent phase pattern moving with respect to the bar that presents a notorious shift around $r = 12$ kpc. For the outermost radii ($r > 15$ kpc), the amplitude values start to be much higher (especially at late times), but we have so few stars per ring that most of them are concentrated in a small range of azimuths and therefore the Fourier representation is likely not accurate enough. Let us emphasize that we see a lopsidedness without constant phase (it changes with the radius), but with a clear cyclical structure.

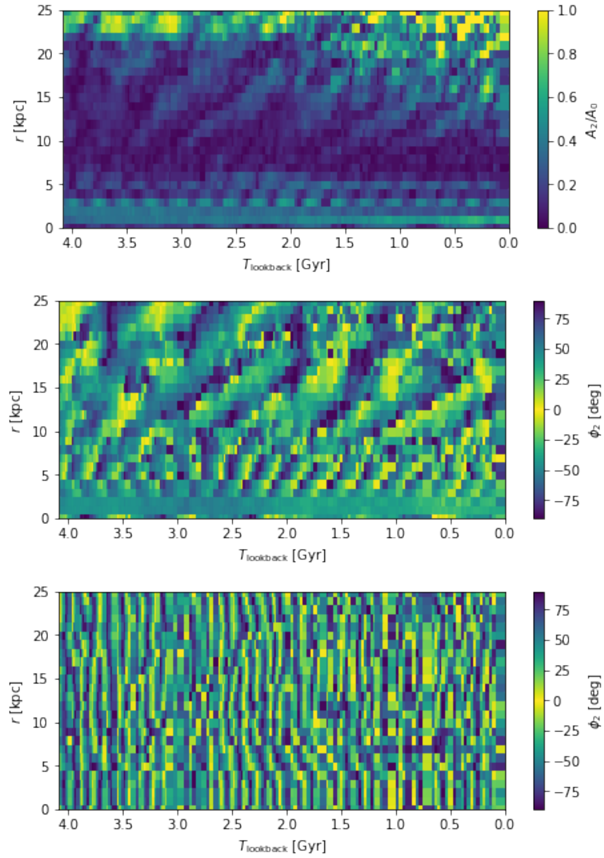

FIG. 5: Same as (Fig. 4) but for mode 2. We use a color bar with different phase range because for this mode the method always returns the minimum phase corresponding to one side of the pattern.

- Mode 2 (Fig. 5): between $r = 0$ kpc and $r = 3$ kpc, we find a bar that can be seen especially well in the fixed bar frame (middle panel) where it has constant phase. At $r =$ 3-4 kpc, there are very regular steps in time in the amplitude. We interpret this as spiral arms, since the phase is not constant with the radius. If it was, it would mean that we have an elliptical distribution. Between $r = 2.5$ kpc and $r = 5$ kpc, the phase of the arms does not connect with that of the bar except for specific times. Thus, these arms rotate at different frequency than the bar. When advancing to intermediate radii, we see a zone of lower amplitudes. Finally, towards external radii and late times, the amplitudes increase, although the noise also increases due to the decrease in stellar density (as in the case of mode 1).

It is interesting to calculate the pattern speed (rotation frequency) of the mode 1 structure since it links with the cause of the pattern itself. Despite that in simulations this is rarely constant over time (for instance, bars typically slow down due to dynamical friction [10]), here we can take it as nearly constant as a first approximation, since it does not vary much in time. Counting the oscillations in a period in the IRF, we obtain a frequency of 33 km/(s·kpc). Analyzing this in detail would allow us to understand interesting aspects (for example, if the spiral arm associated with the mode 1 is a kinematic wave [5]).

Although the analysis that we have just presented has been applied for a certain subgroup of stars, we have also carried it out with a group of older stars (between 5 and 10 Gy). For reasons of extension we do not include the figures or the details, but we highlight that the behavior and patterns obtained are very similar to those observed for our subset despite the fact that, in general, the amplitudes are significantly lower (which can be expected given that older stars respond less to disturbances).

IV. CONCLUSIONS AND DISCUSSION

In this work we have analyzed the temporal evolution of the structure of a simulated MW-type galaxy for each radius. As the results obtained show high complexity, we summarize the main characteristics. Inside the galaxy there is a central bar that makes mode 2 dominate up to $r = 5$ kpc. Mode 1 dominates between 10 kpc and 20 kpc, which we see reflected in a spiral arm that winds around the galaxy and evolves cyclically through time. The galaxies that present this structure are called Magellanic spirals and examples of these would be the Large Magellanic Cloud or NGC 4618. Thus, this work gives us tools to study galaxies that present one spiral arm dominant over the other modes.

Comparing our results with previous studies, we see that our Fourier relative amplitudes of mode 1 come out higher than expected (in [7] these are between 0.3 and 0.5, while ours reach values of up to 1). This may be because we have analyzed a particularly disturbed galaxy, or because they work with observations and, therefore, with the light of the stars, while we work with data obtained by a simulation and, therefore, with the individual simulated particles, which is closer to the mass of the stars, and both results are not directly comparable.

We propose different hypotheses to explain the observed behavior, starting with the disturbance caused by satellites approaching the galaxy over time. To check this, we compare our results with a figure from García-Conde et al., (in prep.) that shows the force exerted on the galaxy by its main satellites as a function of time. Observing the pericenters (moments of minimum satellite-galaxy distance), we see that the orbital periods of the satellites are about 10 times greater than the rotation period calculated for our mode 1. Therefore, we do not see a clear correlation between them and the behavior of the galaxy. However, we cannot rule out the influence of the satellites because this would need a more detailed study since they can have indirect effects (e. g. creating a wake in the main halo that could perturb the disk [7]). Other possible causes are the influence of another main galaxy nearby inside the cosmological box of the simulation (it would affect the distribution of the halo and, therefore, the lopsidedness of the galaxy) or the gas accretion.

As a result of this work, some ideas arise to be studied in the future in order to clarify questions that remain unresolved. Some examples are: studying the pattern speed in depth to determine the nature of the spiral arm; applying the Fourier method to the star velocities since there is a correlation between them and the density of the galaxy; and analyzing the forces exerted by the different agents to infer the repercussion of these on the shape of the halo and the disk, and therefore on the lopsidedness.

Acknowledgments

I would like to sincerely thank my advisor Teresa Antoja for her incredible predisposition, encouragement and guidance. I also want to thank my family for their unconditional love.

[1] Bournaud, F., Combes, F., Jog, C. J., & Puerari, I. 2005, , 438, 507
[2] Ghosh, S., Saha, K., Jog, C. J., Combes, F., & Di Matteo, P. 2021, arXiv e-prints, arXiv:2105.05270
[3] Hu, S. & Sijacki, D. 2018, , 478, 1576
[4] Jog, C. J. 1992, Astrophys. J. , 390, 378
[5] Jog, C. J. & Combes, F. 2009, , 471, 75
[6] Odewahn, S. C., Cohen, S. H., Windhorst, R. A., & Philip, N. S. 2002, Astrophys. J. , 568, 539
[7] Rix, H.-W. & Zaritsky, D. 1995, Astrophys. J. , 447, 82
[8] Roca-Fàbrega, S., Valenzuela, O., Colín, P., et al. 2016, Astrophys. J. , 824, 94
[9] Watts, A. B., Power, C., Catinella, B., Cortese, L., & Stevens, A. R. H. 2020, , 499, 5205
[10] Weinberg, M. D. 1985, , 213, 451
[11] Weinberg, M. D. 1995, , 455, L31